International Journal Of Engineering Research And Development
e- ISSN: 2278-067X, p-ISSN: 2278-800X, www.ijerd.com
Volume 18, Issue 5 (Sep.-Oct. 2022), PP. 12-23

Design Construction and Testing Of a Constant Heat and Aggitation Speed Biodiesel Batch Reactor

[*1]Soja, Y.J., [1]Usman, A.M., [1]Yami, A.M. and [2]Duvuna, G.A.
[1]*Department of Mechanical Engineering, Modibbo Adama University, Yola, Nigeria*
[2]*Department of Mechanical Engineering, Federal Polytechnic Mubi, Adamawa State Nigeria*

ABSTRACT
Temperature and speed of agitation in a batch reactor are parameters that play an important role in the yield of biodiesel. There is a need of maintaining these parameters in the reactor to aid the esterification process. The aim of the study is to design and construct microcontroller and monitoring device for maintaining constant temperature and agitation speed to a12-litter capacity biodiesel batch reactor. Microcontroller PIC18F4520, LM35 temperature sensor, pumps, and valves were used for temperature control. Brushless direct current (BLDC) motor driver (MC33033), and optical encoder mounted on the shaft were used to measure and control the speed of the motor. The performance of the reactor was determined by esterification and transesterification reactions conducted with and without temperature and speed sensors. Speed of agitation and the temperature were taken at five minutes' interval throughout the duration of the reaction processes. Four liters of Khaya-senegalensis oil was reacted with mixture of 3.775 liters of methanol and 37g of H_2SO_4 at 450 rpm for one hour for esterification process. It was reacted with mixture of 1.11liters of methanol and 58.1g of NaOH for 2 hours at 450 rpm for transesterification process. The controller was able to control the speed of agitation of the reactor at 450 $\pm$10rpm and the temperature of the reactor at 55$\pm1^0$C.At this reactor condition, the free fatty acid (FFA) of the oil was reduced from 15.5% to less than 2%(i.e. 88% reduction) and 3.6 liters of biodiesel was obtained(i.e. 90% conversion). It was concluded that constant temperature and agitation speed in the reactor increase the production of biodiesel and reduction in FFA. Also, the microcontroller was able to maintain these parameters within the allowable limit.
Keywords: *Reactor, Biodiesel, Fossil Diesel, Speed, Temperature*

Date of Submission: 22-11-2022 Date of Acceptance: 06-12-2022

I. INTRODUCTION

Fossil fuels are used mainly as a source of energy for transportation, electricity generation and for powering of agricultural machineries. These fuels are non-renewable and responsible for greenhouse gas (GHG) emissions and other particulate matter. Biodiesel fuels are renewable and environmentally friendlier than fossil fuels in terms of reducing exhaust emissions and high biodegradability. Biodiesel is a compound of mono-alkyl esters derived from various types of vegetable oils, lard, waste cooking oil, etc.(1). According Brahma, *et al.* (2), there will be rapid increase in energy demand by 2030 and there will be no fossil fuel enough for human utilization by 2060.Therefore, research in strengthening the methods for utilization of renewable and green energy resources such as sun, wind, hydro, ocean, and tidal for energy generation are vital for human survival. Even though they provide solution to several non-renewable energy problems but biofuels can offer additional solution in replacing the use of fossil fuels. Biofuels are emerging as a good candidate to meet the feature energy demand. Most countries in the world are concerned about the emission of greenhouse gases and the recovery of deforested territory with arable and non-arable vegetation and therefore the production of biodiesel is a good alternative (3). Problems associated with Bio-diesel usage include increase of NO_x exhaust emissions, increased oxidative stability and cold flow properties. Biodiesel has some advantageous features over conventional petrol and diesel such as low viscosity, high flash point, high cetane number, good lubricity, biodegradability, non-toxicity and releases fewer greenhouse gases. It also have lower ignition delay time and high combustion efficiency (2).Its primary advantages are that it is renewable fuel, available, non-toxic and biodegradable (4).It also improves engine performance and reduces net CO_2 emissions by about 70% when compared with conventional diesel fuel (5). It can be used directly in most diesel engines without requiring extensive engine modifications (6).

Vegetable oils are promising fuels because their properties are similar to that of diesel fuels and are produced easily and renewably from crops. Globally, there are more than 350 oil bearing plants that are potential feedstock for biodiesel production (7). Vegetable oils have comparable energy density, cetane number, heat of vaporization and stoichiometric air- fuel ratio with that of diesel fuel. The high viscosity and instability

derived from triglycerides are the most challenging obstacles to the use of vegetable oil directly as diesel fuel. The high viscosity leads to unfavourable pumping and insufficient mixing of fuel with air contributes to incomplete combustion. Several processes have been developed from different studies to resolve the problems in recent years. Such processes include transesterification, pyrolysis, blending with petrol diesel, micro-emulsification with alcohols and hydro treatment (8).

Biodiesel is a diesel fuel produce by trans-esterifying vegetable oils or other materials largely comprising of triglycerides, such as animal fats or used frying oils with monohydric alcohols to give the corresponding mono-alkyl esters (2). Trans-esterification is the most widely used process because of the similarity of the physical characteristics of biodiesel with the existing diesel fuel. It is the most convenient method of producing biodiesel in the presence of a catalyst (9). Vegetable oil is converted into fatty acid alkyl esters (biodiesel) by the reaction of triglycerides with alcohol in the presence of catalyst. The yield of the biodiesel from oil during trans-esterification depends on the reaction condition such as temperature, type and amount of catalyst, alcohol to oil ratio, agitation speed, reaction time, free fatty acid and moisture content of the oil (10; 11).

As reported by Demirbas (12), the most important parameters affecting trans-esterification process in a batch reactor are reaction temperature, speed of agitation, molar ratio of catalyst to oil, molar ratio of alcohol to oil, water content, and fatty acid content of the oil. Reaction temperature and boiling point of alcohol also influences the reaction rate and yield of biodiesel during transesterification. The temperature inside the reactor as reported different researchers ranges between 318 K to 338 K. The boiling point of alcohol is 337K and any temperature higher than this will burn the alcohol and will result in much lower yield biodiesel production (12). There is a need of achieving constant reactor temperature and agitation speed in a biodiesel batch reactor for optimum yield which forms the main thrust of this study. Specifically, the work entails designing and constructing a biodiesel batch reactor, micro controller and monitoring display device. Hence the aim of the study is design and construction of a micro controller and monitoring device for maintaining constant temperature and agitation speed for a biodiesel batch reactor.

II. MATERIAL AND METHODS

The study involves the design, construction and testing of a constant temperature and agitation speed biodiesel batch reactor which comprises of designing and selection of several components. The major components designed include temperature regulating device (which consist of a jacketed vessel that allows for the circulation of hot or cool water) and a stirring mechanism. It also includes hot and cool water supply source (heater), pipes, tubes, pumps, valves and electronic control mechanism.

2.1 MATERIALS

The biodiesel reactor was produced from stainless steel metal sheet (Gauge No. 6) and the reactor was fitted with (brushless direct current) BLDC motor driver, BLDC motor, keypad, liquid crystal display (LCD), Pumps, valves, temperature sensor, optocoupler, microcontroller, electric heater and water tanks. Machines used include lathe, drilling and welding machines. The raw materials used were vegetable oil (*Khaya senegalensis* oil) together with methanol (C_2H_5OH), sulphuric acid (H_2SO_4) and sodium hydroxide (NaOH) in different ratios as catalyst.

2.2 METHODS

The biodiesel batch reactor

The reactor was design and constructed based on standard or studies of Cooker (13). it was subjected to loads such as pressure load, dead weight (the vessel and its content), the external loads (imposed by piping) and attached equipment, etc. The reactor was designed to withstand the worst combination of these loads without failure. The primary stresses arising from these loads are shown in Fig.1.

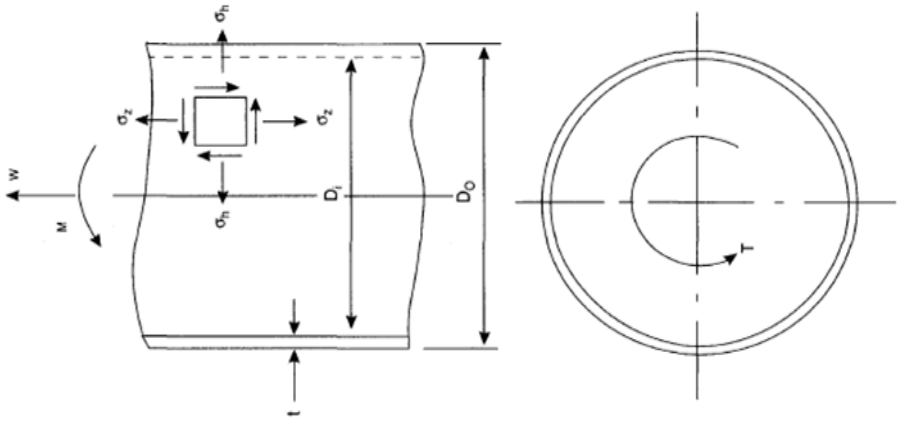

Figure 1: Stress in a Cylindrical Shell under Combine Loading (14)

Vessel stresses design

The longitudinal (σ_n) and circumferential (σ_z) stresses, acting on the vessel due to internal or external pressures are calculated usingeq. 1 and 2 respectively (14):

$$\sigma_n = \frac{PD_i}{4t} \quad (1)$$

$$\sigma_z = \frac{PD_i}{2t} \quad (2)$$

For a cylindrical shell, the minimum thickness required to resist internal pressure can be determined from eq. 2. If D_i is the internal diameter and e is the minimum thickness required, the mean diameter will be $D_i + e$. Substituting for D_i in eq. 2, and computing for e we have (15):

$$e = \frac{PD_i}{2f - P_i} \quad (3)$$

Where P_i= internal pressure of the cylinder, N/m^{2}and f = design stress, N/m^2. The direct stress, σ_w, due to the weight of the vessel, its content and any attachments is given by eq.4.The dead weight of the vessel, *W*, is given by eq. 5.

$$\sigma_W = \frac{W}{\pi(D_1 + t)t} \quad (4)$$

$$W = 240 C_V D_m (H_v + 0.8 D_m) t \quad (5)$$

Where t = wall thickness of the reactor(mm), D_i= internal diameter of the reactor(mm), D_m= the mean diameter of the reactor can be using$D_m = (D_i + tx10^{-3})\ (m)$, H_v = vertical hight of the reactor (mm) and $C_V = 1.08$ (factor accounting for the weight of nozzles, man ways, internal support, etc.).

The principal stresses acting on the vessel are given by eq.6 and 7respectively;

$$\sigma_1 = \frac{1}{2}\left[\sigma_n + \sigma_z + \sqrt{(\sigma_n - \sigma_z)^2 + 4\tau^2}\right] \quad (6)$$

$$\sigma_2 = \frac{1}{2}\left[\sigma_n + \sigma_z - \sqrt{(\sigma_n - \sigma_z)^2 + 4\tau^2}\right] \quad (7)$$

Maximum shear stress theory states that failure will take place in a complex system when the maximum shear stress reaches the value of the shear yield stress in simple tension (14). For a system of combined stresses there are three stress maxima$\tau_1, \tau_2\ and\ \tau_3$ given by eq.8, 9and 10, respectively.

$$\tau_1 = \frac{\sigma_1 - \sigma_2}{2} \quad (8)$$

$$\tau_2 = \frac{\sigma_2 - \sigma_3}{2} \quad (9)$$

$$\tau_3 = \frac{\sigma_3 - \sigma_1}{2} \quad (10)$$

Where σ_1 , $\sigma_2\ and\ \sigma_3$ are the principal stresses

Shaft and power design

In reactor design, the shaft of the reactor is responsible for the transmission of power from the electric motor to the fluid via the flat blade impellers. The design of the shaft consists primarily of determination of the correct shaft diameter to ensure satisfactory strength and rigidity when the shaft is rotating and transmitting power

under different operating and loading conditions(15).Eq. 11 shows relationship between the rotation, transmission and load conditions.

$$\frac{T}{J} = \frac{\tau}{r} = \frac{G\theta}{l} \quad (11)$$

Where$\theta =$ angle of twist, degree, $T =$ total resisting torque(Nm), $J =$ polar moment of inertia(m^4), $\tau =$ maximum shearing stress(N/m^2), $G =$ modulus of rigidity (N/m^2), $r =$ radius of the shaft(m) and $l =$ length of the shaft(m).

The shaft diameter and the power transmitted by the shaft (P) are related by eq.12 and 13respectively (15).

$$J = \frac{\pi}{32} d^4 \quad (12)$$

$$P = \frac{2\pi NT}{60} \quad (13)$$

Where T is the applied torque (Nm) and N is the shaft rotational speed (rev/min). The design equations used to determine the thickness of the flat ends are based on the analysis of stresses in the flat plates.The geometrical proportions of a standard agitation tank shown in Fig.2are reported inCoker(13) can be computed using eq. 14.

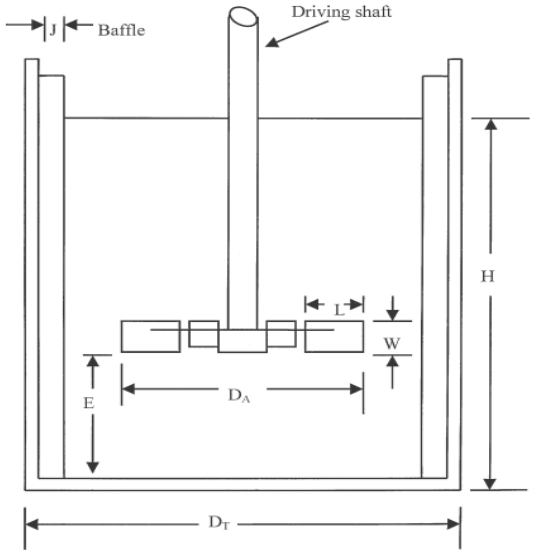

Figure 2: Geometry of a standard agitation tank system (13)

The power consumed by an agitator depends on the size of the agitator and the density and viscosity of the fluids being mixed. For a stirrer thank reactor with the following dimensions: diameter (D_T), impeller width (W) and the liquid depth (H), having a Newtonian liquid of density (ρ), viscosity (μ) being agitated by an impeller of diameter(D_A) which rotates at a speed (N) as shown in Fig.2, the power (P) required for the agitation of the liquid can be expressed as a function of the following dimensionless numbers:

$$N_P = KR_e{}^b Fr^c \quad (14)$$

The dimensionless parameters power number N_p, Reynolds number R_e and Froude number F_r in eq.14are defined ineq.15 and 17:

$$N_P = \frac{P}{D_A{}^5 N^3 \rho} \quad (15)$$

$$R_e = \frac{D_A{}^2 N\rho}{\mu} \quad (16)$$

$$F_r = \frac{N^2 D_A}{g} \quad (17)$$

Where P = shaft power(W) (input power), K = a constant, dependent on the agitator type, size and the agitator tank geometry, $\rho =$ fluid density(kg/m^3), $D_A =$ agitator diameter(m), $g =$ gravitational acceleration($9.81 m/s^2$).For $R_e < 300$, the constant K and the exponent's b and c are described in Coulson, *et al.* (16).

The value of Reynolds number (R_e) determines whether the flow is laminar or turbulent and is a significant group affecting the power consumption. The power consumed by an agitator at various rotational speeds and physical properties (viscosity and density) can be determined from the Power number correlation (eq. 14).By calculating the Reynolds number (R_e) for mixing (eq. 16) and reading the Power number (N_p) from the power curve the power consumed by the agitator can be calculated using eq.18(13).The torque delivered to the fluid by an impeller from its speed and power drawn are related as ineq.19(17):

$$P = N_P \rho N^3 D_A^5 \quad (18)$$

$$T = \frac{P}{2\pi N} = \frac{N_P \rho N^2 D_A^5}{2\pi} \quad (19)$$

2.3 Control components design and specification

Design of the controller

The design of the controller was carried out in two stages namely: Hardware development stage and software development stage respectively. The hardware development consists of designing the hardware for temperature and speed control of the system, selection of various components used in the design, and production of PCB board. The power needed to operate this system requires transformation and rectification. Full wave rectification was used to provide the DC voltage required. The power requirements of the system are as follows;

i. 24V, 2.4A DC for DC motor.
ii. 12V, 2A DC for valves and pumps.
iii. 5V, 1A DC for control unit, display unit and temperature sensor unit, and the optical encoder.

The voltage from the main supply 230V A.C. was stepped down by a transformer to 9V, 12 V and 24V respectively using a diode bridge. The 9V passes through voltage regulator LM317 to give 5volts DC.

Optical encoder and BLDC motor driver (MC33033)

An optocoupler CNY17 was used in this designed as a speed sensor. It requires 5V DC power supply. It consists of LED and a photo transmitter encapsulated in one package and is interphase to the microcontroller and the motor. The optocoupler is being powered by 5V power supply. The driver requires an operating voltage of 10 to 30V, 6.25V reference voltage capable of supplying sensor power and a high current driver that can control external 3-phase MOSFET Bridge. These requirements are met by the 24V power supply to power the device.

Keypad and liquid crystal display (LCD)

The keypad is connected to the microcontroller through pins RD0 – RD7 and is powered by the microcontroller. The LCD module used in this work requires a supply voltage of 5V, maximum current of 3mA and power is 15mW. These requirements are also met by the 5V regulated power supply.

Electric heater, temperature sensor and microcontroller

A 230V AC, 1000W electric heater was used in the design for heating water in the hot water tank. The heater is connected to 230V AC from the main supply and is being switched by the relay as shown in Fig.3.

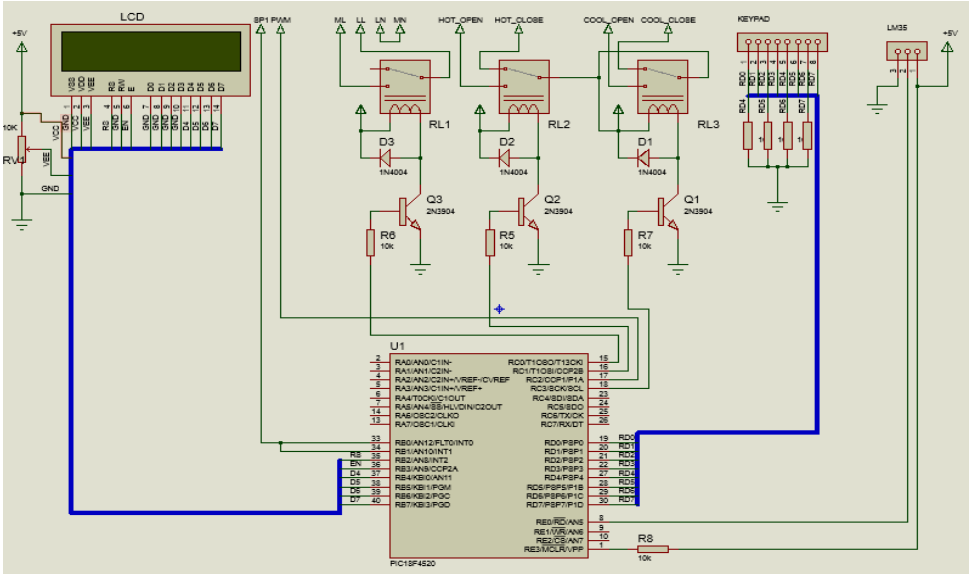

Figure 3: Circuit diagram for the temperature and speed control of the biodiesel reactor

The operating voltage of LM35 ranges from 4V to 30V but in this study 5V is supplied to it, a maximum current is less than 60µA and a rated power of0.3mW. These requirements are met by the 5V regulated power supply. The LM35 temperature sensor is inserted inside the reactor and its output temperature is in milli volts. This output temperature is converted into corresponding digital data using inbuilt A/D converter in the microcontroller. The key pad and the LCD are interfaced with the microcontroller. The value of the output temperature is displayed on the LCD. The circuit diagram for connection of the temperature sensor to the microcontroller is shown in Fig.4. The microcontroller requires supply voltage of 5V, maximum current of 25mA and power of 625mW which are met by the 5V regulated power supply.

Pumps and valves

The specifications of the centrifugal pumps which were used in this study for the circulation of hot and cool water respectively into the reactor include rated current of 3A, rated voltage of 12V DC, discharge of 6.5litres/minutes, flow head of 2m and operating temperature between 0 to 90^{o}C. The specifications of the motorized valves used in this study for the control of hot and cool water circulation in and out of the reactor are normally open and motorized valve type, rated current of 3A, voltage of 12V DC and Pressure of 1.0 MPa. These power requirements were met by the use of 12V regulated power supply source from the transformer.

Design of BLDC motor and speed controller

The BLDC motor used in this design require an operating voltage of 24V DC. This requirement is meet by the 24V power supply. Fig.4 described the design of BLDC motor driver circuit. The speed control mechanism was designed using microcontroller PIC18F4520, BLDC motor driver (MC33033) and optical encoder.

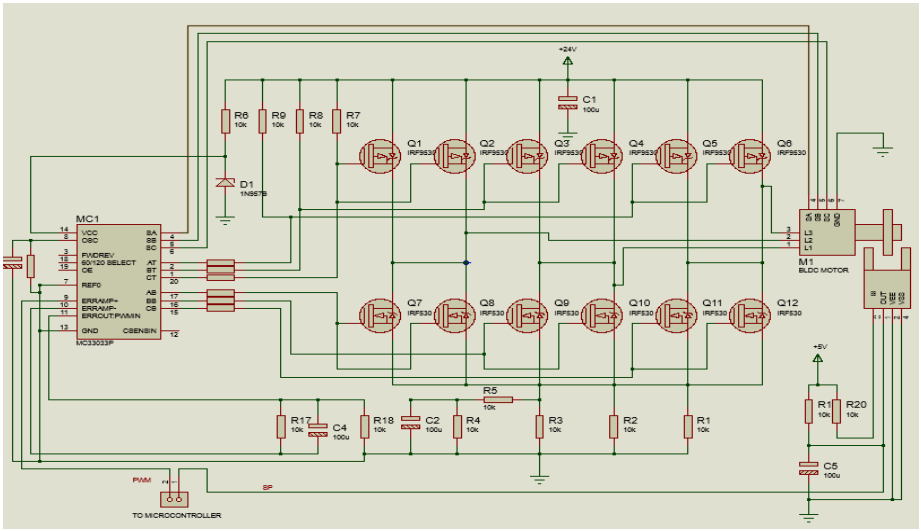

Figure 4; Circuit diagram of BLDC motor driver

The Optical encoder is mounted on the BLDC motor shaft and measures the speed of the motor and sends it the microcontrollers in form of voltage and current. The microcontroller computes the speed of the motor by sensing the voltage and current from the optical encoder, and compares the speed of the motor with the set speed (input or desired speed from the keypad), and generates an error signal which is used to vary the PWM of the motor signal that is used to control the switches of the three-phase bridge of the motor driver (refer to Fig. 5 and 6 for the schematic block diagram of a biodiesel reactor speed and temperature controller). The motor driver produces three phase voltages to the three stators of BLCD motor and the MOSFET switches are triggered with respect to the rotor positions. Only two switches are used one in the upper bank and the other in the lower bank are conducting at any given rotor position. When the actual speed of the BLDC motor is lower than the set speed the microcontroller will automatically increase the PWM and hence the rpm of the motor will increase, also when the actual speed of the BLDC motor is higher than the set speed the microcontroller will automatically reduce the PWM and hence the rpm of the motor will reduce, thus controlling the voltage supply to the BLDC Motor driver.

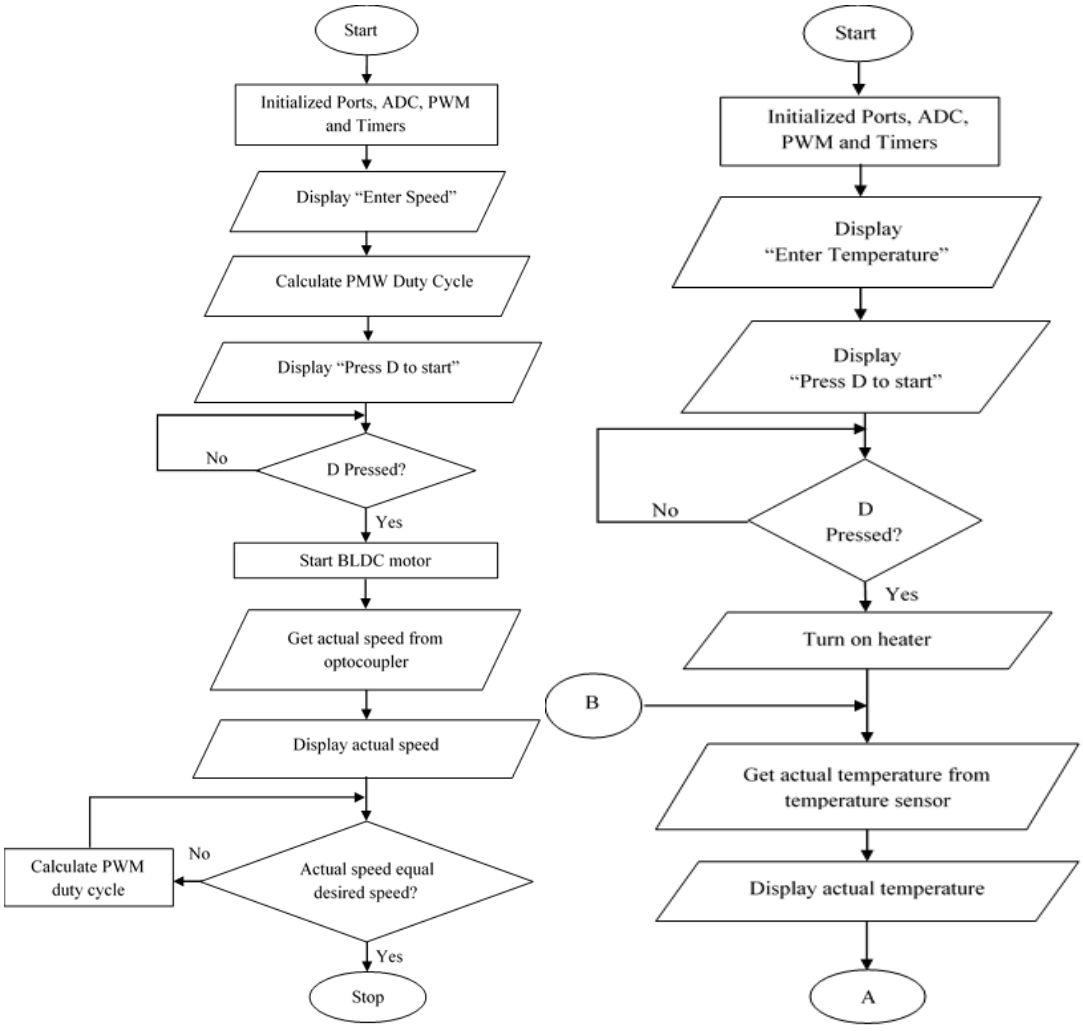

Figure 5: Flow chart for (a) Speed controller (b) Temperature controller initial flow

Software implementation

Micro C (version 5.6) was used to program the microcontroller in a high-level language called C for the purpose of speed and temperature control. Microcontroller acts as the brain of the whole speed and temperature control. It receives the desire input (start, stop, desired speed and desired temperature) from the user through the key pad that is connected to the microcontroller. These inputs are ASCII characters 'a', 'b', etc. and they are easily received by the microcontroller. An algorithm was developed for speed and temperature control and represented by flowcharts in Fig.5 and 6 to make the microcontroller to read the input and act as required. The flowchart was translated into C programming language and compiled to hexadecimal format using Micro C software development tool.

Reactor open loops speed and temperatures

Testing of the biodiesel reactor was carried out by determining both the open loop (uncontrolled) and controlled speed characteristics of the reactor during the process of esterification and the transesterification reaction. The open loop (uncontrolled) speed characteristics of the reactor's motor was determined by assembling the reactor with pumps, valves, DC motor and a heater connected to the control unit. But the optocoupler (speed sensor) was not connected to the microcontroller. The microcontroller does not receive any feedback signal from the optocoupler. The LCD displays the open loop speed of the reactor's motor. Also for the uncontrolled temperature, temperature sensor was not connected to the microcontroller; instead a thermocouple was inserted into the reactor and was used to measure the temperature inside the reactor. The thermocouple was also connected to a digital meter which directly measures and displays the uncontrolled temperature of the reactor. While for the controlled speed and temperature of the reactor, the speed temperature sensors were connected to the microcontroller and the speed and temperature inside the reactor were displayed by the LCD.

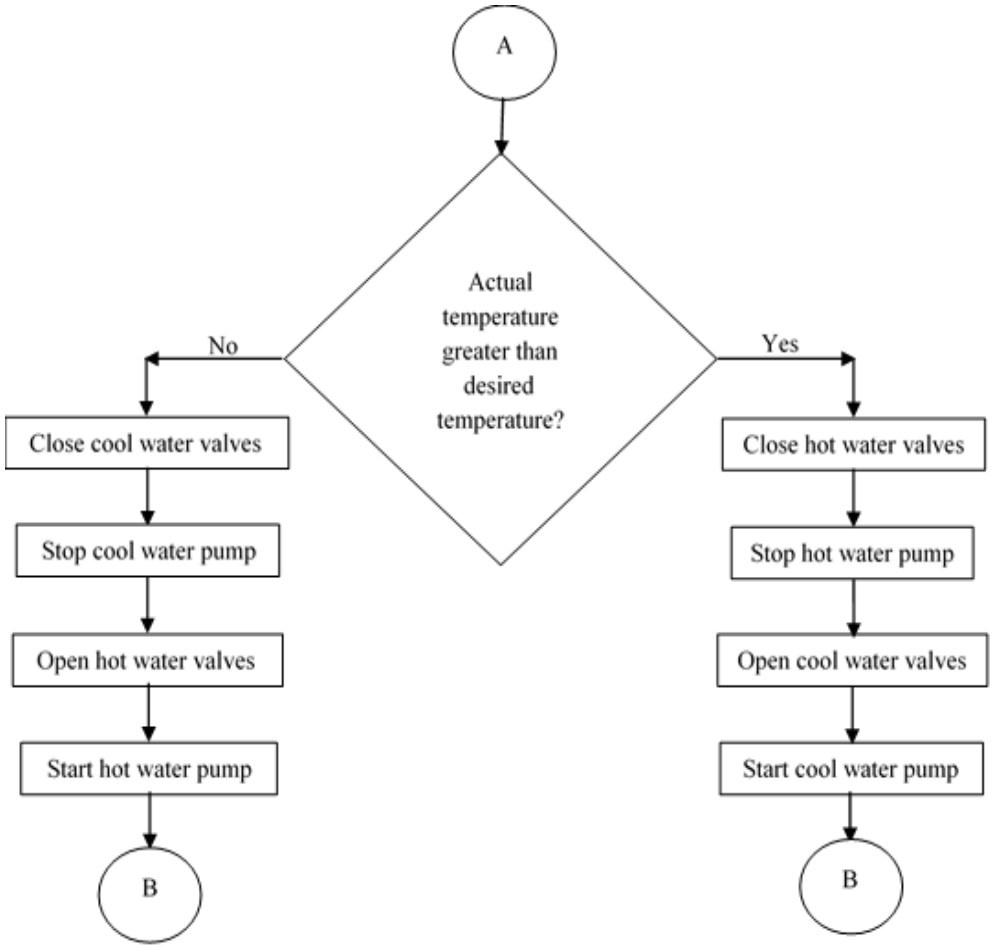

Figure 6: Completion of flow Chart for Temperature Controller

Efficiency of complete reactor

The efficiency of the complete reactor can be calculated using power ratios eq. 20 or biodiesel yield eq. 21.

$$\eta = \frac{P_{output}}{P_{input}} \quad (20)$$

$$\eta = \frac{Quantity\ \ of\ raw\ material\ \ used}{Quantity\ \ of\ Biodiesel\ \ produced} \quad (21)$$

Descriptions of the reactor

The biodiesel reactor as shown in Fig.7 consist of a cylindrical vessel of diameter 270mm, height 270mm inserted into another cylindrical vessel of diameter 290mm and height 270mm to form a jacketed reactor. Water circulates through the annular space between the jacket and vessel walls for heating and cooling of content of the reactor through heat transfer. Circulation baffles were installed in the annular space between the jacket and vessel walls to increase the velocity of water flowing through the jacket and to improve heat transfer coefficient. Hot water is supplied to the annular space between the jacket and vessel walls through a connecting horse from the hot water tank which is heated by a 1000W heater. In addition, cool water is also supplied to the annular space between the jacket and vessel walls through a connecting horse from the cool water tank. The cool water is used to regulate the temperature of the content of the reactor. Hence whenever the temperature of the reactor exceeds the desired temperature the system trips-off. The stirrer is a flat blade turbine made up of six blades and connected to brushless direct current (BLDC) Motor. The BLDC Motor rotates the stirrer which creates homogeneity of the reactant through mixing the contents of the reactor thereby enhancing heat and mass transfer. The reactor has four baffles placed at equidistance on the reactors wall to provide smooth mixing of the reactants in the reactor and to avoid vortex formation and turbulence during the mixing process. Baffles also ensure good heat transfer in the reactor (1).

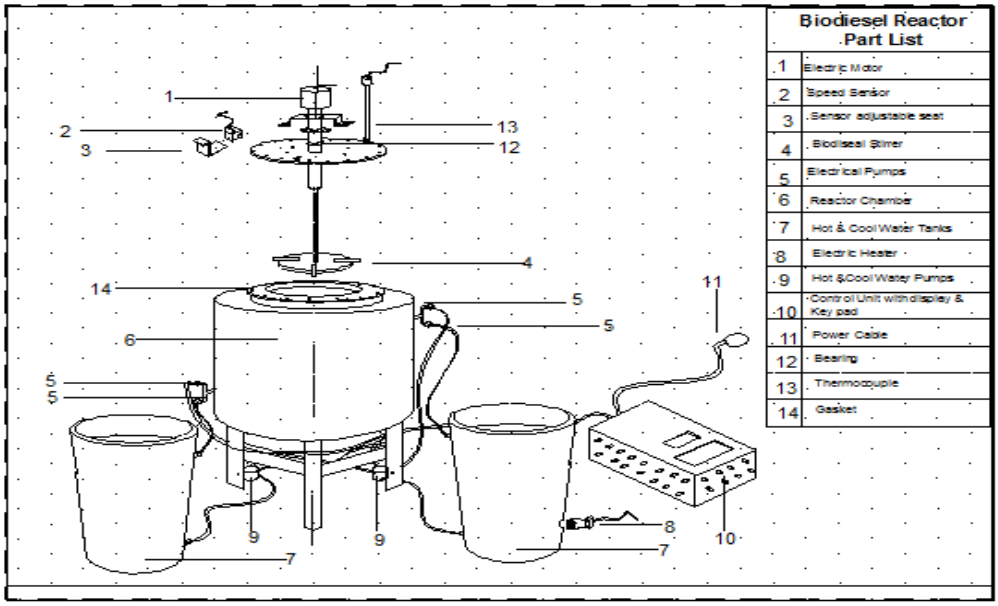

Figure 7: Pictorial view of the biodiesel reactor

2.4 Experimentation

Esterification reaction

To initiate the esterification process, 4 liters of *Khaya-senegalensis* oil was allowed to react with 3.775litres of methanol and 37g of sulphuric acid (H_2SO_4)as describe in Cooker (13). The reaction at agitation speed of 450 rpm and temperature of 50^{o}C was maintained throughout the reaction time of one hour in the reactor. The esterification of the oil by the acid catalysis is necessary whenever the free fatty acid (FFA) level is greater than 1% as can be seen from the physico-chemical properties of *Khaya-senegalensis* oil in Table 1.

Table 1. Physico-chemical properties of *Khaya-senegalensis* oil

Property	**Values**
Colour	Light brown
Free fatty acid	7.5 %
Acid value	14.925 mg.KOH/g
Peroxide value	65 mg/kg
Saponification value	105 mg KOH/g
Iodine value	41.24 g/100/
Kinematic viscosity @ 40 ^{o}C	2.52^{o}C
Density @ 30 ^{o}C	0.905 g/cm^3
Flash point	230 ^{o}C

Transesterification reaction

Transesterification of the *Khaya senegalensis* oil was carried out by preheating the oil products from the first step to 50^{o}C and poured into the reactor. The preheating of the oil will make the oil free from water, since any water or moisture in the system will consume some of the catalyst and slow down the transesterification reaction (18).Mixtures of methanol and catalyst (1.11liters of methanol and 58.1g of NaOH) were heated to 50^{o}C before adding to the heated oil products in the reactor. The contents of the reactor were heated and stirred at 450 rpm and temperature of 50^{o}C was maintained throughout the reaction time of two hours. The speed of agitation of the reactor and the temperature inside the reactor as displayed by the LCD were recorded after an interval 5 minutes. The mixture was allowed to settle over night before separating the glycerol layer to get the methyl ester of the fatty acid at the top. The biodiesel was then washed with warm water to remove lye, soaps, methanol and other impurities that are in the biodiesel. A straw-yellow and a cloudy liquid layer was formed, the cloudy liquid was drained out. The biodiesel was heated to 55^{o}C on a hot plate to allow the remaining water to evaporate, and was finally filtered using filtering paper (19). The volume of the biodiesel obtained was measured and recorded.

III. RESULT AND DISCUSSION

3.1 Result of FFA reduction

The average result of the free fatty acid (FFA) level reduction from the *Khaya senegalensis* oil in percentage before and after the esterification reaction are shown inFig.8

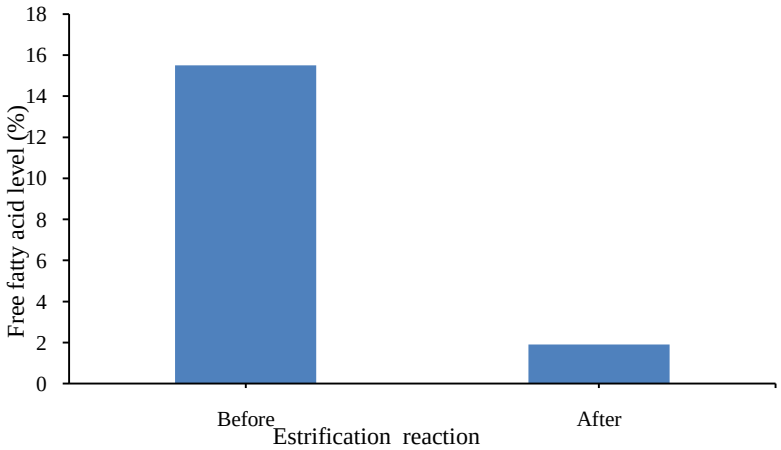

Figure 8: Free fatty acid content before and after esterification

It was observed from Fig. 8 that during the esterification reaction in the presence of sulphuric acid, an agitation speed of 450 rpm and reaction period of one hour, the free fatty acid of the oil was reduced from 15.5%to less than 1.9%. These give about 88% reduction efficiency. The use of acid catalyst is required to maximize the biodiesel yield from the transesterification whenever the FFA level is greater than 1%.Therefore, during transesterification The result shows efficiency of FFA reduction of 87.7%. The result is consistent with the findings of Daniyan, *et al*. (17) and Hosseini, *et al*.(20).

3.2 Results for reactor agitation speed

Fig.9a show the variation of the agitation speed of the reactor against time under controlled and uncontrolled conditions during the esterification and transesterification processes.

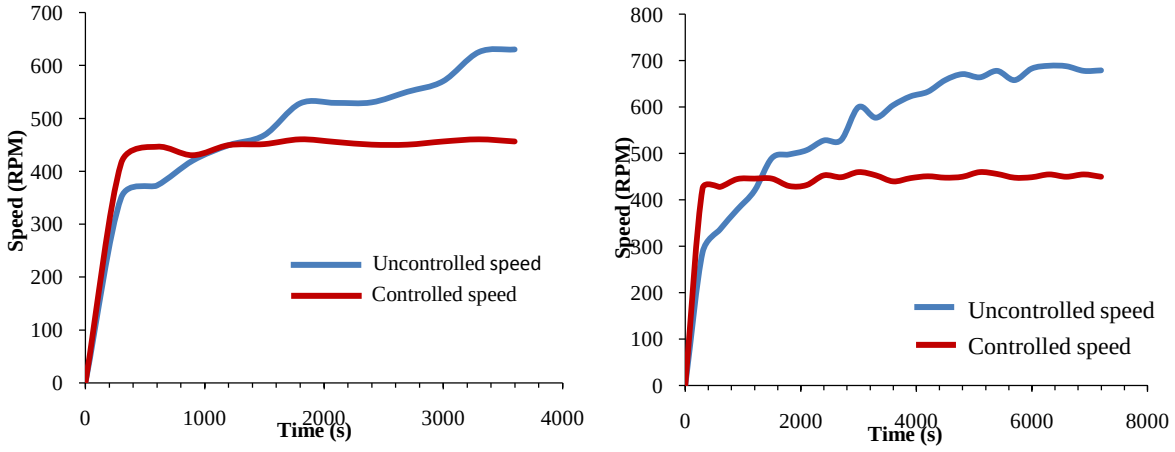

Figure 9. Variation of reactor speeds with time during (a) esterification process (b) transesterification process

For the uncontrolled speed in Fig. 9a, the graph shows a continuous increase in speed of the reactor as the esterification reaction proceeds. The speed reaches a maximum value of 630 rpm after 3600s. While for the controlled speed shown inFig.9a, the plots show a rapid rise from zero to about 415 rpm after a short period of 300s, and flattens out at about 450 rpm to 460 rpm, for the remaining period of test duration (i.e. 450±10 rpm). For the uncontrolled speed shown inFig.9b, the graph shows a continuous increase in speed of the reactor as the transesterification reaction proceeds, and reaches a maximum value of 689 rpm after 6300s. While for the controlled speed also shown inFig.9b, the plots show a rapid rise in agitation speed from zero to about 425 rpm after a short period of 600 s, and flattens out initially between425 rpm and 445 rpm and finally settle after about 1000 s and above it ranges between 450 to 460 rpm for the remaining period of test duration (i.e. 450±10 rpm).

3.3 Reactor open loop temperature characteristics

Fig.10described the temperature of the reactor against time under controlled and uncontrolled conditions during the esterification and transesterification processes respectively.

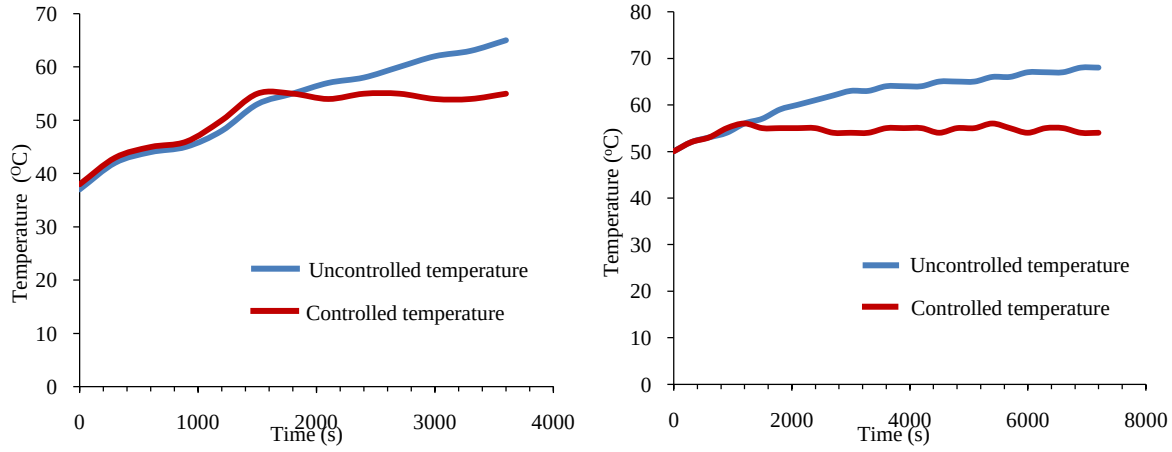

Figure 10.Variation of reactor temperatures with time during (a) esterification process (b) transesterification process

For the uncontrolled temperature as can be seen from Fig. 10a, the graph illustration demonstrated that as the esterification reaction proceeds, a continuous increase in temperature of the reactor was achieved. The temperature builds up in the reactor continuous beyond the set temperature of 55^{o}C i.e. to 65^{o}C after 3600s. For the case of controlled reactor temperature shown inFig.10a, a temperature rises from 38^{o}C to 55^{o}C after 1800s was recorded. This temperature subsequently stabilizes between 54^{o}C to 56^{o}C for the remaining experimental period up to 3600s (i.e. 55±1^{o}C). For the uncontrolled temperature in the transesterification process Fig.10b, the graph illustration demonstrated that as the transesterification reaction proceeds, a continuous increase in temperature of the reactor was achieved. The temperature builds up in the reactor continuous beyond the set temperature of 55^{o}C to a maximum of 68^{o}C after 7200s. For the case of controlled reactor temperature Fig.10b, a temperature rises from 50^{o}C to 55^{o}C after 900s was recorded. This subsequently stabilizes between 54^{o}C to 56^{o}C for the remaining experimental period up to 7200s (i.e. 55±1 ^{o}C).

3.4 Result of biodiesel yield

During the transesterification process, when the oil products from the esterification was reacted with the catalyst about an average of 3.6 ltr of biodiesel was obtained as can be seen from Fig. 11.

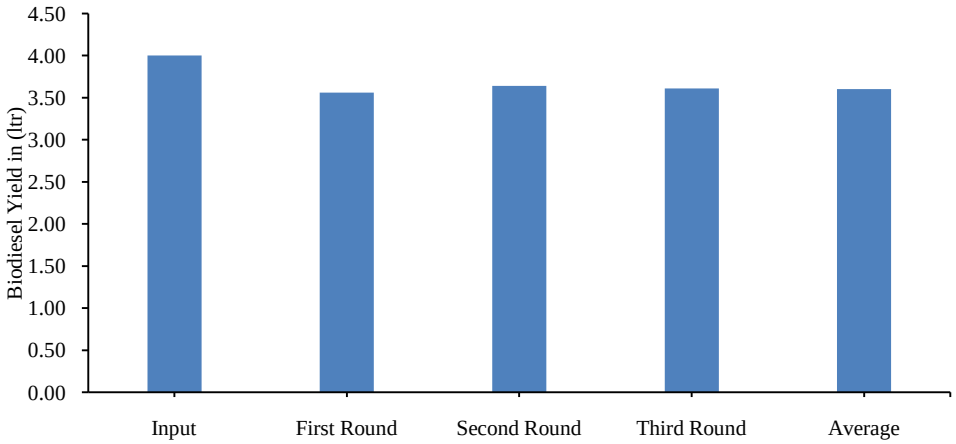

Figure 11; Average Biodiesel yield during transesterification

The results in Fig. 11 show an average of about 90% biodiesel conversion from *Khaya senegalensis* oil by the use of the improvised reactor. Wongjaikham, *et al.* (1)also obtained a conversion of 82.53% at 65^{o}C from refined palm oil.

IV. CONCLUSION

From the foregoing, it could be concluded that the design of a temperature and speed control mechanism for a locally fabricated 12 liters capacity biodiesel reactor was achieved. From the experimentation, it was concluded that the speed of the reactor was controlled between 450 rpm to 460 rpm(i.e. 450±10 rpm)

during both the esterification and transesterification processes. Also, the temperature was maintained between 54^{o}C to 56^{o}C (i.e. 55±1 ^{o}C) respectively. During this constant speed and temperature, the free fatty acid was reduced by 88% during esterification process. The biodiesel yield provides up to 90% conversion from *Khaya senegalensis* oil during the transesterification process.

REFERENCES

[1]. Wongjaikham, W., Wongsawaeng, D., Ratritsai, V., Kamjam, M., Ngaosawm, K., Kiatkittipong, W., Hosemann, P. and Assabumrungrat, S., 2021. "Low-cost alternative biodiesel production apparatus based on house hold food blender for continuous biodisel production for small communities," Nature,

[2]. Brahma, S., Nath, B., Basamatary, B., Das, B.,Saikia, P., Pabir, K. and Basamatary, S., 2022. "Biodiesel production from mixed oils: A sustainable approach towards industrial biodiesel production," Chemical Engineering Journal Advancess, vol. 10,

[3]. Parez-Salinas, C. F., Nunez-Nunle, D. F., Sanaguano-Selguero, H. R. and Samchez-Quinschuela, L. F., "Design and construction of a batch reactor with external recirculation to obtain biodiesel from residual oil frying under subcritical conditions," Ignenius, vol. 25, pp. 32-40, 2021.

[4]. Knothe, G. and Steidley, K. R., "Kinematic viscosity of biodiesel fuel components and related compounds: influence of compound structure and comparison to petro diesel fuel components," Fuel, vol. 84, pp. 1059-1065, 2005.

[5]. Buhari, M., Danbature, W. L., Mazakir, M. M. and Abubakar, B. A., "Production of biodiesel from baobob seed oil," Greener Journal of Agricultural Sciences, vol. 4, no. 2, pp. 22-26, 2014.

[6]. J. V. Garpen, "Biodiesel Processing and Production," Fuel Processing Technology, vol. 86, no. 10, pp. 1097-1107, 2005.

[7]. Atabani, A. E., Mafijur, M., Maskuki, H. H., Badruddin, I. A., Chang, W. T., Chenz, S. F. and Qouk, S. W., "A study of production and characterization of manketts (Ricinodendron rautonemii) methyl ester and its blends as a potential feed stock," Biofuel Research Journal, vol. 4, pp. 139-146, 2014.

[8]. Shaofeng, G., Akira, S., Mingliang, S. and Eika, W. Q., "Hydra-treating of Jatropha oil over alumina based catalysts," Journal of Energy and Fuels, vol. 26, pp. 2394-2399, 2012.

[9]. Rashid, A. B. and Kader, M. F., "Performance analysis of an automated biodiesel processor," Environmental and Climate Technologies, vol. 26, no. 1, pp. 84-97, 2022.

[10]. Endalew, A.K., Kiros, Y. and Zanzi, R., "Heterogeneous catalysis for biodiesel production from Jathropha Curcus," Journal of Energy, vol. 36, pp. 2693-2700, 2011.

[11]. Meher, L. C., Dhamagadda, V. S. S. and Naik, S. N., "Optimization of Alkali-Catalyzed transesterification of Pongomia pinna oil for production of biodiesel," Bio-resources Technology, vol. 97, pp. 1392-1397, 2006.

[12]. A. Demirbas, "Importance of biodiesel as transportation fuel," Energy Policy, vol. 35, no. 39, pp. 4661-4670, 2009.

[13]. R. K. Sinnot, Chemical Engineering Design, New Delhi: Butterworth Heinemann, 1999, pp. 791-877.

[14]. Kurmi, R. S. and Gupta, J. K., A Text Book of Machine Design, 4th ed., New Delhi: Eurasia Publishing Company, 2009, pp. 370-382.

[15]. A. K. Cooker, Modelling of Chemical Kinetics and Reactor Design, 5th ed., Houston Texas USA: Gulf Publishing Company, 2004.

[16]. Coulson, J. M., Richardson, J. F., Buckhurst, J. R. and Harker, J. H., Chemical Engineering: Fluid Flow, Heat and Transfer, 6th ed., vol. 1, New Delhi: Butterworth heinemann, 1999.

[17]. Daniyan, I. A., Adeodu, A. O., Dada, O. M. and Aribidara, A. A., "Design of a small scale biodiesel processor," Journal of Emerging Trend in Engineering and Applied Science, vol. 4, no. 4, pp. 576-580, 2013.

[18]. Topare, S., Patil, K. D., Kherkar, S. V. and Inamder, N., "Laboratory scale batch reactor design fabrication and its application for biodiesel production," Techno-social, vol. 78, no. 3, pp. 819-828, 2021.

[19]. Mondala, A., Liang, K., Toghiani, H. and Hernaudez, R., "Biodiesel production by in situ transesterification of municipal primary and secondary slugs," Bio-resource Technology, pp. 1203-1210, 2009.

[20]. Hosseini, M., Nikbakht, A. M. and Tabatababaei, M., "Biodiesel production in batch reactor equipped with Helical Ribbon-l like Agitation," Modern Applied Science, vol. 6, no. 3, 2012.